Journal of Electrochemical Science and Technology
Vol. 2, No. 2, 2011, 110-115
http://dx.doi.org/10.5229/JECST.2011.2.2.110

Journal of Electrochemical Science and Technology

Effect of the TiO_2 Nanotubes in the Photoelectrode on Efficiency of Dye-sensitized Solar Cell

Md. Mahbubur Rahman[a], Hyun-Seok Son[b], Sung-Su Lim[b], Kyung-Ho Chung[b], and Jae-Joon Lee[a,b,†]
[a]*Department of Advanced Technology Fusion, Konkuk University, Seoul 143-701, Korea*
[b]*Department of Applied Chemistry, Konkuk University, Chungju 380-701, Korea*

ABSTRACT :

The effect of TiO_2 nanotube (TNT) and nanoparticle (TNP) composite photoelectrode and the role of TNT to enhance the photo conversion efficiency in dye-sensitized solar cell (DSSC) have investigated in this study. Results demonstrated that the increase of the TNT content (1-15 %) into the electron collecting TNP film increases the open-circuit potential (V_{oc}) and short circuit current density (J_{sc}). Based on the impedance analysis, the increased V_{oc} was attributed to the suppressed recombination between electrode and electrolyte or dye. Photochemical analysis revealed that the increased J_{sc} with the increased TNT content was due to the scattering effect and the reduced electron diffusion path of TNT. The highest J_{sc} (12.6 mA/cm^2), V_{oc} (711 mV) and conversion efficiency (5.9%) were obtained in the composite photoelectrode with 15% TNT. However, J_{sc} and V_{oc} was decreased for the case of 20% TNT, which results from the significant reduction of adsorbed dye amount and the poor attachment of the film on the fluorine-doped tin oxide (FTO). Therefore, application of this composite photoelectrode is expected to be a promising approach to improve the energy conversion efficiency of DSSC.

Keywords: TiO_2, Nanotube, Nanoparticle, Dye-sensitized solar cell, Recombination

Received May 20, 2011 : Accepted June 5, 2011

1. Introduction

Titanium dioxide (TiO_2) film with mesoporous nanostructures and anatase crystalline polymorph has been applied as photoelectrode for dye-sensitized solar cell (DSSC) due to their oxygen vacancies, titanium interstitials, high surface area, and high relativities.[1)] Moreover, TiO_2 is abundant in nature and nontoxic. In spite of these advantages, the structural disorder of TiO_2 nanoparticles (TNP) film leads to the elongation of electron colleting path and ultrafast scattering of free electrons, and thereby increase the probability of recombination at the interface between TiO_2 and electrolyte or dye.[2,3)] This reduces the electron collection efficiency and results in hindering the enhanced energy conversion efficiency of DSSC.[4)] Among the strategies including passivation layer and composite nanostructures to overcome this limitation, one dimensional (1-D) TiO_2 nanostructures (e.g. nanotube, nanowire, and nanorod) is the most promising approach.[5-7)]

The application of highly ordered TiO_2 nanotube (TNT) arrays in DSSC has attracted enormous interest since the pioneering work of Grimes and co-workers in 2001.[8,9)] Varghese *et al*[10)] reported that the use of TNT has the photoconversion efficiency of over 12.25% and the quantum efficiency of over 80% under 320-400 nm illumination. The recombination at TNT alone film was suppressed with the increase of the collection efficiency due to the directional electron movement.[1,5)] However, little high

†Corresponding author. Tel.: +82-43-840-3580
E-mail address: jjlee@kku.ac.kr

energy conversion efficiency of DSSC based on TNT was reported, which was mainly due to the reduction of dye adsorption on the low surface area of TNT compared to that of TNP. Therefore, the composite film of TNT and TNP can be applied as photoelectrode, which is expected to increase the electron collection efficiency, amount of dye loading, as well as reduce the recombination. Furthermore, scattering effect is also expected in the composite film because of the big size of TNT.[11,12)]

This research discussed the effect of TNT/TNP composite photoelectrode with different composition of synthesized TNT into commercially available TNP on the performance of DSSCs. The optimal concentration of the synthesized TNT into TNP for the improved DSSCs performance with keeping the morphology of TNT was proposed based on the optical, photoelectrochemical, and electrochemical impedance spectroscopic (EIS) characteristics.

2. Experimental

2.1. Preparation of TNT/TiO_2 paste

TNT was synthesized by mixing 5 g of TiO_2 nanoparticles (P-25, Degussa, Germany) in 200 mL of 10 M NaOH, followed by drying at 110°C for 15 h. After drying, the precipitate was collected and washed with water for several times and treated with 0.1 M HNO_3 for 2 hours. The acid treated TNT sample was washed with de-ionized water (DI) water, ethanol, and then dried at 50°C. The detailed procedure for the preparation of paste was described in our previous work.[13)] Briefly, 1.0 g of the acetyl-acetone pretreated TNP (TTP-20N, ENBKOREA Co., Ltd., Korea) and as-synthesized TNTs were mixed (TNT composition 0%, 0.1%, 0.3%, 0.5%, 1%, 3%, 5%, 10%, 15%, and 20%) separately with 2 mL of distilled water, 0.05 mL of acetyl-acetone, 5 mL of 10% ethanolic solution of hydroxypropyl cellulose (HPC), and 5 mL of ethanol with vigorous stirring and stirred for 12 h. Finally, ethanol was evaporated slowly at 50°C with constant stirring to get the viscous paste in which cellulose was 50% (w/w).

2.2. Fabrication of DSSCs

The TNT/TNP films on fluorine doped tin oxide (FTO, Pilkington, 8 Ω/□ , USA) were prepared by doctor blade method and sintered for 30 min in an electric muffle furnace in presence of air at 500°C. The sintered films were dipped into a 0.4 mM ethanolic solution of *cis*-diisothiocyanato-bis(2,2'-bipyridyl-4,4'-dicarboxylato) ruthenium(II) bis-tetrabutylammonium (N719) dye for 15 h. The counter electrodes were prepared by spin coating of 5 mM ethanolic solution of chloroplatinic acid hexahydrate ($H_2PtCl_6 \cdot 6H_2O$) on FTO and sintered in an electric muffle furnace at 380°C for 20 min. The dye loaded photoelectrodes (active area *ca.* 0.2 cm^2) and platinized counter electrodes were sandwiched with 50 μm thick Surlyn film as a spacer and sealing agent under the condition of 110°C for 10 min. The electrolyte solution having composition of 0.6 M 1,2-dimethyl-3-propylimidazolium iodide (DMPII), 0.1 M LiI, 0.1 M I_2, and 0.5 M 4-*tert*-butylpyridine (*t*BP) in 3-methoxypropionitrile (MPN) was injected into the cell through the drilled holes on the counter electrode. They were sealed up with a piece of transparent scotch tape.

2.3. Instrumentation

The morphology and structure of the synthesized TNT and TNP (TTP-20N, ENBKOREA Co., Ltd., Korea) were characterized by using a transmission electron microscope (TEM, Jeol, JEM-1200 Ex II, Japan), and an X-ray Diffractometer (Philips, X'pert, Netherland) using Cu K_α radiation of $\lambda = 0.15406$ nm in the scan range $2\theta = 10\text{-}90°$. Surface morphologies of the photoelectrodes were characterized by scanning electron microscope (SEM, Hitachi S-3000N, Japan). UV-Visible transmission spectra of the photo-electrodes were measured by a UV-Vis spectrophotometer (Perkin Elmer, Lambda 35, USA).

A solar simulator (Polaronoix® K201, McScience, Korea) furnished with a 200 W Xenon lamp to generate simulated light of AM 1.5 was used for photovoltaic measurements of the DSSCs. A photovoltaic power meter (Polaronoix K101 LAB20, McScience, Korea) was used to measure the current density-voltage (*J-V)* curves. The incident light intensity was adjusted to 100 $mWcm^{-2}$ (1 sun) by a standard mono-Si solar cell (PVM 396, PV Measurement Inc, USA), which was certified by National Renewable Energy Laboratory (NREL,USA). Incident photon to current conversion efficiency (IPCE) spectra was measured by IPCE measurement system (McScience, K3100 Spectral IPCE Measurement System, Polaronix®) with 300 W Xenon light source. The intensity of the incident monochromatic light was also calibrated with the same standard mono-Si solar cell (PVM 396, PV Measurement Inc, USA). Electrochemical impedance spectra (EIS) was measured by an impedance analyzer (IM6ex, Zahner-Elektrik GmbH & Co. KG, Germany) in the dark over a frequency range of 10^5-0.1 Hz with the ac amplitude of 10 mV at V_{oc} of each cell.

3. Results and Discussion

3.1. Characterization of TNT

Fig. 1 shows the TEM image of the TiO_2 nanoparticles (25 nm) and the synthesized TNT. It was clearly observed that the synthesized TNTs were in nanotube forms having very narrow size distribution (lengths 80-200 nm, diameter 15-20 nm). The XRD patterns of the synthesized TNT before and after calcinations at 500°C are depicted in Fig. 2, which shows the phase transition from amorphous to crystalline by the calcinations of the TNTs.[14] It is noteworthy that the broad peak at 22° reflects the amorphous nature of the sample holders and in reality a small quantity of samples was available for the measurements.

3.2. SEM and Transmittance Characteristics of the photoelectrodes

Fig. 3 shows the cross sectional SEM images of different

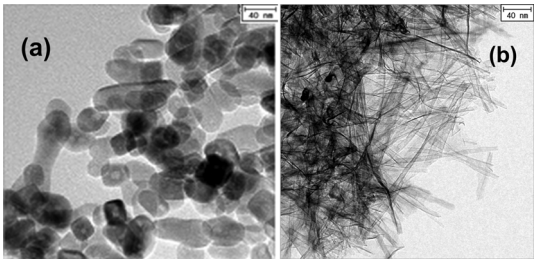

Fig. 1. TEM image of (a) TNP and (b) TNT.

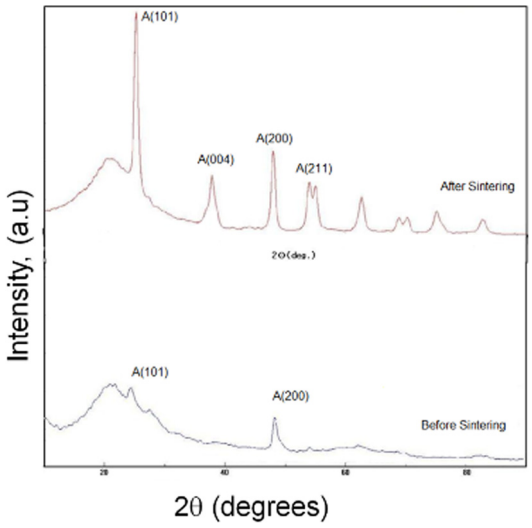

Fig. 2. XRD pattern of the synthesized TNT powder before and after sintering.

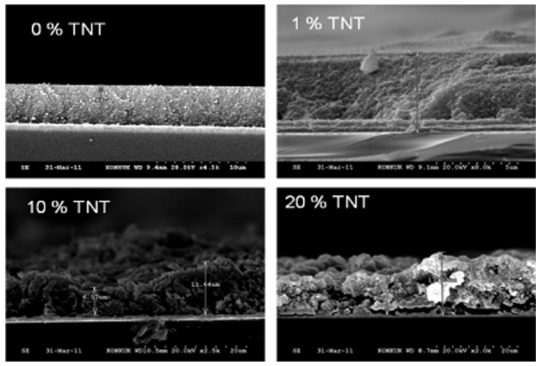

Fig. 3. Cross-sectional SEM image of different percent of TNT mixed TNP photoelectrode after sintering.

percentages of TNT/TNP photoelectrodes. It was observed that with the increase of the content of TNT, the porosity and inhomogeneity of the photoelectrode increased, while the compactness of the films decreased and thickness of the photoelectrode increased gradually. The alterations of these physical properties of the films were attributed to the interfacial characteristics of TNT and TNP. Kontos *et al.*[15] reported that the increased inhomogeneity and the decreased compactness of the film reduced the DSSCs performance, while the increased porosity is very important for enhanced photoconversion. Therefore, investigation of optimum percent of TNT into TNP is indispensible.

Fig. 4 shows that the transmittance decreased at every wavelength (350-800 nm) with the increase of the content of TNT in the photoelectrodes. Especially, the significant reduction of the transmittance was observed for 10, 15, and 20% of TNT content, indicating the amount of absorbed photon in the cases prominently increased compared to the other ratio of TNT/TNP in photoelectrodes. Also it means that the TNT/TNP conditions occurs a scattering effect of the light, and prolonged the optical path.[1,16] This optical property of the high TNT content into TNP is favorable for the excitation of the adsorbed dyes, which can result in enhancing the photo-current.

In order to confirm the scattering effect, we have performed the IPCE measurement of all the DSSCs as shown in Fig. 5. No significant change of IPCE was observed for the TNT content of 0.1-1% in the wavelength ranges from 280 to 800 nm. On the other hand, for TNT content of 3-20%, a clear increase of the EQE (%) in the range of 600-750 nm was due to the scattering effect of TNT while a decrease of the EQE (%) was observed in the range of 400-600 nm due to the low dye adsorption, which is the pronounced absorp-

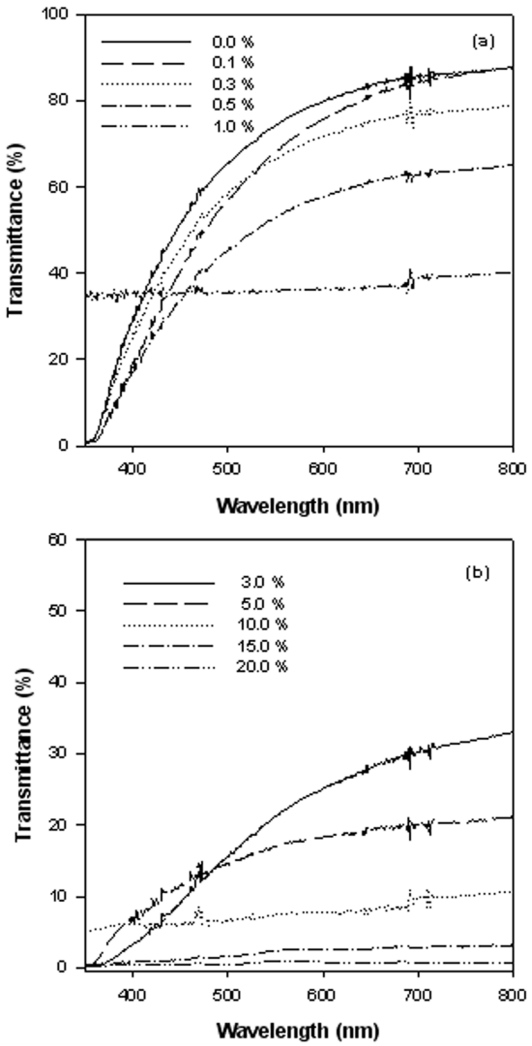

Fig. 4. Change of transmittance spectra by TNT contents mixed in TNP photoelectrode.

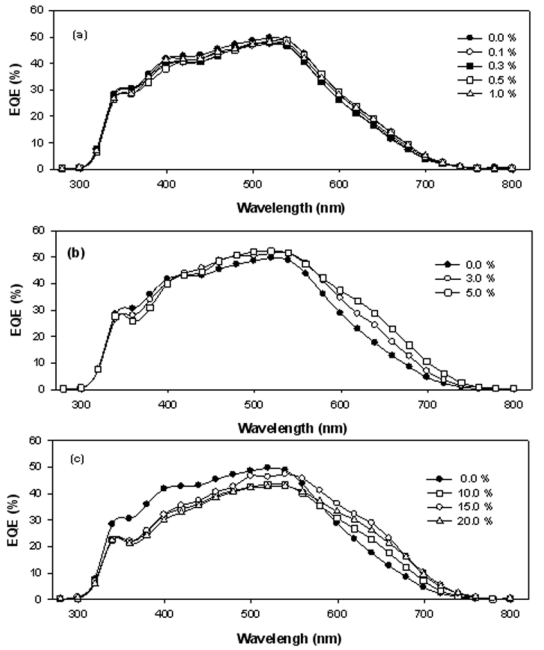

Fig. 5. Change of the incident photon to current conversion action spectra by altering the content of TNT into TNP.

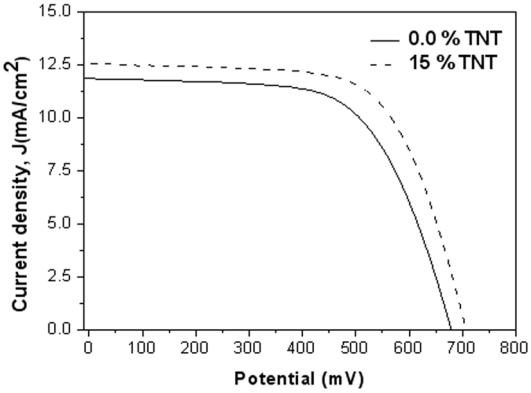

Fig. 6. Comparison of current density-voltage characteristics of 0% and 15% of TNT content DSSCs.

tion window of N719 dye.[2,17] On considering both photon absorbance data (Fig. 4) and IPCE data (Fig. 5), the greatest enhancement of J_{sc} was expected for 15 % TNT content.

3.3. Photovoltaic characteristics of the DSSC photoelectrodes

As shown in Table 1, short circuit current density (J_{sc}) and open circuit potential (V_{oc}) increased for 1-15% TNTs contained TNP photoelectrodes compared to the TNP only photoelectrode. Generally, with the increases of the TNT content the surface area of the photoelectrodes and the adsorbed dye amount decreased.[18] Therefore, the increase of J_{sc} for the 1-15% TNT/TNP photoelectrodes were attributed to the improved charge collection efficiency, directional electron movement, and the increased light harvesting efficiency as expected from the transmittance data (Fig. 4). The decreased J_{sc} for 20% TNT photoelectrode resulted from the relatively high inhomogeneity of the film, and decreased binding strength of the film with FTO (Fig. 3). Even though, the transmittance trend for 20% TNT case was similar to that of 15% TNT,

the yielded photon to electron decreased significantly that is responsible for the reduced dye adsorption.

The fill factor (FF, %) and efficiency (η, %) change was also followed the same trend of J_{sc} for the DSSCs of 1-15% TNT. DSSC of 15% TNT content showed the highest energy conversion efficiency (η = 5.86%) compared to reference (0% TNT) (η = 5.08%) and their comparative current density-voltage (J-V) curve is shown in Fig. 5.

The kinetics of electron transfer processes at the photoelectrode|electrolyte interface was studied by electrochemical impedance spectroscopy (EIS). The EIS spectra are presented in the Bode phase plot and the calculated kinetic information of the TNT/TNP electrodes are summarized in Fig. 7 and Table 1, respectively. In the order of decreasing frequency, the high frequency (first) peak corresponds to the charge transfer at the Pt-counter electrode, and the uncovered FTO|electrolyte interface; the mid-frequency (second) peak corresponds to the diffusion-recombination at the photoelectrode; and the low frequency (third) peak is related to the ionic diffusion process in the electrolyte, which is often merged with mid-frequency peak as in our data. The rate of back electron transfer to I_3^- at the interface of TNT/TNP electrodes| electrolyte ($k_{T/E}$) was estimated from the mid-frequency peak as $\omega_{max} = k_{T/E}$.[19] With the increase of the TNT content, the measured $k_{T/E}$ values decreased up to 15% of TNT content and increased for 20% TNT compared to 0% TNT. The decreases of the $k_{T/E}$ strongly suggest the lower recombination in TNT/TNP electrodes compared to TNP only.[20] The recombination rate for 20% TNT electrodes in little higher than other TNT/TNP (1-15%) electrodes but lower than TNP electrode only. This might be due to the weak alignment and poor networking of the 20% TNT/TNP with FTO.

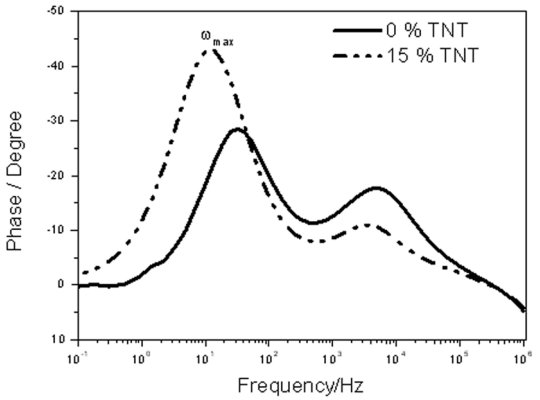

Fig. 7. Bode plots from electrochemical impedance measurement of 0% and 15% of TNT content DSSCs under dark condition.

Table 1. Photovoltaic and kinetic parameters of different DSSCs photoelectrodes

TNT content (%) in TiO_2 film	V_{oc} (mV)	J_{sc} (mA/cm^2)	FF (%)	Efficiency, η (%)	$k_{T/E}$ (s^{-1})
0	678	11.9	63.2	5.1	32.7
0.1	701	11.1	64.3	5.1	21.1
0.3	702	10.8	64.3	4.9	21.2
0.5	700	10.9	64.0	4.9	21.3
1	700	12.0	63.4	5.4	20.1
3	700	12.4	64.3	5.6	18.7
5	702	12.4	63.4	5.5	16.1
10	706	12.4	65.0	5.6	14.5
15	711	12.6	66.0	5.9	12.1
20	695	11.4	65.0	5.1	21.3

4. Conclusions

In the study, the effect of the incorporation of TNT into TNP photoelectrode was investigated based on the electrochemical and photochemical perspectives. The highest energy conversion efficiency was observed in 15% TNT incorporated TNP film in terms of best J_{sc}, V_{oc}, and FF. Additionally, the presence of TNT in the photoelectrode could abate the recombination of electrons at the interface between TiO_2 and electrolyte or dye. TNT gives obviously the effect to enhance the photon to electron conversion efficiency, which results in increased J_{sc}. The results in this study suggested that the composite photoelectrode can be applied to enhance the energy conversion efficiency in DSSCs by the scattering effect, suppressed recombination, and directional electron movement.

Acknowledgements

This research was financially supported by the Ministry of Education, Science Technology (MEST) and National Research Foundation of Korea (NRF) through the Human Resource Training Project for Regional Innovation. It was also supported by the New & Renewable Energy of the Korea Institute of Energy Technology Evaluation and Planning (KETEP) grant funded by the Korea government Ministry of Knowledge Economy (No. 2009301001002A) and the Ministry of Knowledge Economy(MKE) and

Korea Institute for Advancement of Technology(KIAT) through the Research and Development for Regional Industry (70006123).

References

1. J.-J. Lee, M. M. Rahman, S. Sarker, N. C. Deb Nath, A.J. S. Ahammad, and J. K. Lee, in Composite materials for medicine and nanotechnology edited B. Attaf, Intech, Croatia, 181 (2011).
2. Z. S. Wang, H. Kawauchi, T. Kashima, and H. Arakawa, *Coord. Chem. Rev,* **248**, 1381 (2004).
3. D. Gong, C. A. Grimes, O. Varghese, W. Hu, R. S. Singh, Z. Chen, and E. C. Dickey, *J. Mater. Res.* 16, 12, 3331 (2001).
4. T. Peng, A. Hasegawa, J. Qui, and K. Hirao, *Chem. Mater.*, **15**, 2011 (2003).
5. J. M. Macak, M. Zlamal, J. Krysa, and P. Schmuki, *Small*, **3**, 300 (2007).
6. Z. Miao, D. Xu, J. Ouyang, G. Guo, X. Zhao, and Y. Tang, *Nano Lett.*, **2**, 717 (2002).
7. X. Peng, and A. Chen, *J. Mater. Chem.*, **14**, 2542 (2004).
8. G. K. Mor, K. Shankar, M. Paulose, O. K. Varghese, and C. A. Grimes, *Nano Lett.*, **6**, 215 (2006).
9. K. Zhu, N. R. Neale, A. Miedaner, and A. J. Frank, *Nano Lett.*, **7**, 69 (2007).
10. O. K. Varghese, M. Paulose, K. Shankar, G. K. Mor, and C. A. Grimes, *J. Nanosci. Nanotechnol.*, **5**, 1158 (2005).
11. W. E. Vargas, *J. Appl. Phys.* **88**, 4079 (2000).
12. H. J. Koo, J. Park, B. Yoo, K. Yoo, K. Kim, and N. G. Park, *Inorg. Chim. acta* **361**, 677 (2008).
13. D.-W. Seo, S. Sarker, N. C. Deb Nath, S.-W. Choi, A. J. S. Ahammad, J.-J. Lee, and W.-G. Kim, *Electrochim. Acta*, **55**, 1483(2010).
14. G. Cerrato, L. Marchese, and C. Morterr, *Appl. Surf. Sci.*, **70-71**, 200(1993).
15. A. I. Kontos, A. G. Kontos, D. S. Tsoukleris, M.-C. Bernard, N. Spyrellis, and P. Falaras, *J. Mater. Process. Tech.*, **196**, 243(2008).
16. B. Brüggemann, J. A. Organero, T. Pascher, T. Pullerits, and A. Yartsev, *Phys. Rev. Lett.*, **97**, 208301 (2006).
17. B. Wenger, M. Grtzel, and J.-E. Moser, *J. Am. Chem. Soc.*, **127**, 12150 (2005).
18. A. Hagfeldt, G. Boschloo, L. Kloo, and H. Pettersson, *Chem. Rev.*, **110**, 6595 (2010).
19. M. Adachi, M. Sakamoto, J. Jiu, Y. Ogata, and S. Isoda, *J. Phys. Chem. B.*, **110**, 13872 (2006).
20. K. Zhu, E. A. Schiff, N.-G. Prak, J. van de Lagemaat, and A. J. Frank, *Appl. Phys. Lett.*, 80, **4**, 687 (2002).